

**Friedel oscillations and superconducting gap enhancement by impurity scattering**Matthias Stosiek,<sup>1</sup> Clemens Baretzky<sup>2,3</sup>, Timofey Balashov,<sup>2</sup> Ferdinand Evers,<sup>4</sup> and Wulf Wulfhekel<sup>2</sup><sup>1</sup>*Physics Division, Sophia University, Chiyoda-ku, Tokyo 102-8554, Japan*<sup>2</sup>*Physikalisches Institut, Karlsruhe Institute of Technology, Wolfgang-Gaede Strasse 1, 76131 Karlsruhe, Germany*<sup>3</sup>*Freiburg Materials Research Center (FMF), University of Freiburg, Stefan-Meier-Strasse 21, 79104 Freiburg, Germany*<sup>4</sup>*Institute of Theoretical Physics, University of Regensburg, 93040 Regensburg, Germany*

(Received 11 July 2021; revised 28 February 2022; accepted 7 March 2022; published 8 April 2022)

Experiments observe an enhanced superconducting gap over impurities as compared to the clean-bulk value. In order to shed more light on this phenomenon, we perform simulations within the framework of Bogoliubov–de Gennes theory applied to the attractive Hubbard model. The simulations qualitatively reproduce the experimentally observed enhancement effect; it can be traced back to an increased local density of states at the Fermi energy in the metal close to the impurity site. In addition, the simulations display significant differences between a thin [two-dimensional (2D)] and a very thick [three-dimensional (3D)] film. In 2D pronounced Friedel oscillations can be observed, which decay much faster in 3D and therefore are more difficult to resolve. Also, this feature is in qualitative agreement with the experiment.

DOI: [10.1103/PhysRevB.105.L140504](https://doi.org/10.1103/PhysRevB.105.L140504)**I. INTRODUCTION**

A nonmagnetic charged impurity in a metal at low temperatures is screened by Friedel oscillations in the particle density [1]. A related effect was predicted more than five decades ago in conventional superconductors in the presence of a nonmagnetic impurity, where the superconducting gap shows an oscillatory response [2]. The cause of both phenomena is the presence of a sharp Fermi surface in these systems. The description of such a response in the superconducting system is considerably more complex than in the noninteracting case. This is due to the self-consistency requirement, as it arises in the mean-field description of an interacting system [3]. When translational symmetry is broken, the nonlinear nature of mean-field Hamiltonians severely limits analytical approaches, but also numerical simulations are challenging; for pioneering works, see Refs. [4,5].

While analytical progress has been made [2,6–10], the analytical form of the response of the superconducting gap is known only in the case of an impurity in the bulk of a three-dimensional (3D) system [2,7]. Numerical studies [3,7,10–12] on the other hand were limited to small system sizes and key properties, such as the spatial decay of the response, have not been analyzed quantitatively.

**II. EXPERIMENTAL MOTIVATION**

To map local variations of the density of states due to scattering, i.e., Friedel oscillations, scanning tunneling microscopy (STM) in ultrahigh vacuum (UHV) is the ideal approach [13]. At low enough temperatures, it also allows determination of the local superconducting gap  $\Delta$ . Local scatterers were created by short Ar-ion sputtering of a clean bulk Al(111) sample. Ions hitting the surface produce defects, mostly implanted Ar [14] acting as pure potential scatterers without spin. At the base temperature of the STM of  $\approx 25$  mK

[15], spectra of the voltage-dependent differential conductance  $dI/dU$  were recorded using nonsuperconductive W tips.

The experimental situation concerning the Friedel oscillations around an implanted Ar impurity is illustrated in Fig. 1(a). Clearly, Friedel oscillations are visible around the defects [14]. Figure 1(b) displays a two-dimensional (2D) map of  $\Delta(x, y)$  near a defect appearing as a depression. Interestingly, the superconducting gap is enhanced near the impurity site [see Fig. 1(c)] for local spectra of the minimal and maximal gap]. A similar gap enhancement is also observed in measurements adopting Fe adatoms as impurities (see Appendix). Figure 1(d) shows the  $z$  position of the STM tip as a function of distance from the center of a defect that shows up as a protrusion. In the topography, clear Friedel oscillations are found followed at larger distances by a fall back of the elevation to that of the plane surface. Their period of the oscillations is with  $\approx 0.9$  nm, in good agreement with the literature [16,17]. Note that the Al bands can be described as free electrons but with a Fermi wave vector in the second and third Brillouin zone [18], which leads to backfolding of the periodicity of the Friedel oscillations. The  $dI/dU$  spectra obtained along the same line from the defect encoded in grayscale are displayed as well. Black corresponds to vanishing  $dI/dU$  inside the gap, while the coherence peak appears bright. Clearly, the gap is significantly enhanced atop of the defect. Upon moving away from the defect, the gap decreases with slight oscillations and reaches the clean value some 5 nm away from the defect as evidenced by the fitted values of  $\Delta$ . Note that the variations are laterally much finer than the coherence length of Al of  $1.6 \mu\text{m}$  at this temperature [19] and happen on the length scale of the variations in the density of states.

Concerning numerical studies of gaps near bulk impurity sites, the published numerical data exhibit local decreases [3,7,10–12] relative to the unperturbed gap; the systematics

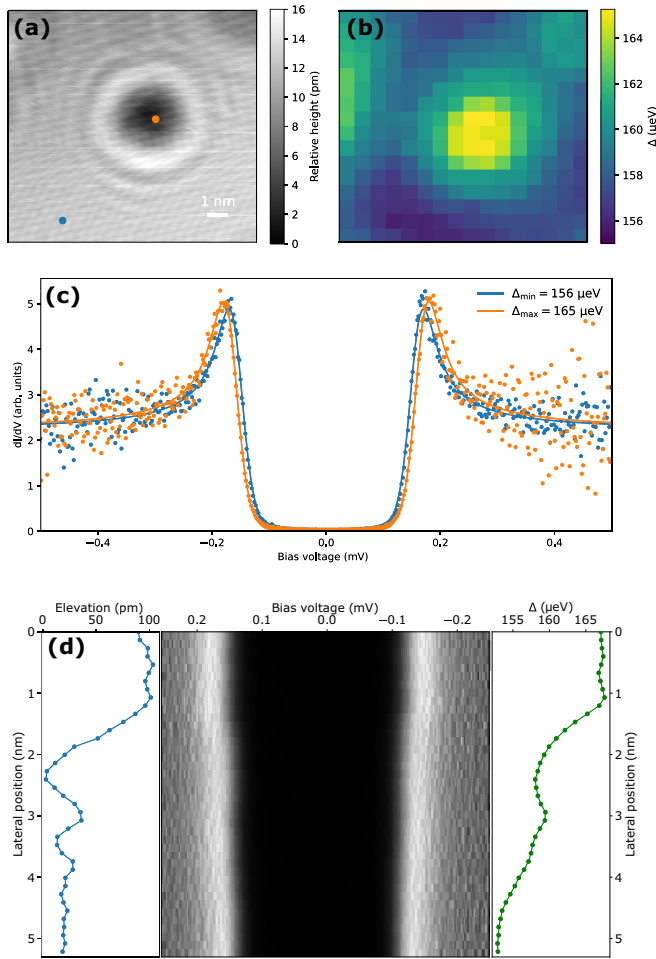


FIG. 1. (a) STM topography of an Al(111) surface with a buried defect after mild  $\text{Ar}^+$  bombardment appearing as a depression. (b) Superconducting gap  $\Delta$  obtained by fitting  $dI/dU$  spectra recorded as a function of lateral position. (c) Examples of local  $dI/dU$  spectra of maximal and minimal  $\Delta$  recorded at positions indicated in (a). Tunneling parameters (a)–(c):  $I = 0.5$  nA,  $U = 0.4$  mV. (d) Change of the  $z$  position, i.e., tip elevation, with distance to the surface defect appearing as a protrusion together with grayscale encoded  $dI/dU$  recorded and the fitted superconducting gap  $\Delta$ . Tunneling parameters:  $I = 8$  nA,  $U = 2$  mV; further experimental details are given in the Appendix.

has not yet been analyzed. These theoretical predictions are in contrast to the experimentally observed enhancement for surface defects.

### III. THEORY

Motivated by the measurements shown in Fig. 1, we have performed numerical simulations of Friedel oscillations in thin (2D) and thick (3D) superconducting films in different system sizes. We work with a tight-binding model parametrized for an adatom on an aluminum substrate, adopting  $s$ -wave superconductivity on the Bogoliubov–de Gennes level. For comparison, earlier studies did not consider adatoms but substitutional atoms in the bulk or near surfaces. Our choice is motivated by the typical arrangement in STM measurements.

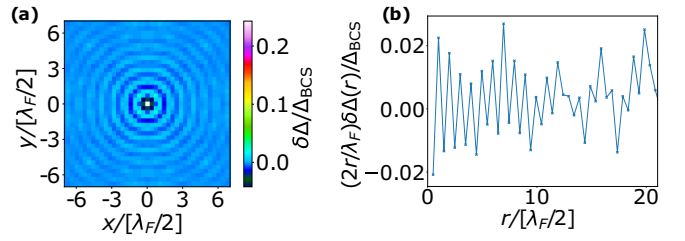


FIG. 2. (a) Spatial map of the response of the pairing amplitude of a 2D superconductor to an impurity located at the origin. (b) Response of the pairing amplitude along the surface diagonal multiplied by the distance from the impurity  $r$  in units of the lattice constant  $a$ . (Parameters: filling  $n = 0.2$ ,  $U = 1.6$ ,  $V_{\text{imp}} = -0.06t$ ,  $\lambda_F/2 \approx 2.85a$ .)

Our most important conclusions are twofold: First, the gap enhancement may be understood as a consequence of the local density of states (LDOS) at the Fermi energy underneath the impurity being increased as compared to the unperturbed surface. Second, depending on the film thickness, Friedel oscillations exhibit a qualitatively different behavior with a  $1/r$  envelope for 2D and a decay considerably faster than  $1/r^2$  in 3D. Our findings thus explain the most striking features seen in experiment (Fig. 1).

*Model and method.* We study the Hubbard model with attractive interaction  $U$  dressed with an impurity realized as an extra site (“adatom”) with scattering potential  $V_{\text{imp}}$ ; if not otherwise stated, we choose  $V_{\text{imp}} = -0.06t$ . The impurity strength has been chosen to model the difference in work function of Fe and Al. The adatom is modeled as a potential impurity, due to the absence of a free spin in experiment (see Appendix).

The model is solved on square (2D) and cubic (3D) lattices on the mean-field level, i.e., within the Bogoliubov–de Gennes (BdG) approximation treated with full self-consistency and stipulating  $s$ -wave pairing; as a consequence, the pairing amplitudes  $\Delta(\mathbf{r})$  and  $n(\mathbf{r})$  are inhomogeneous in space. The interaction strength  $U$  is tuned so that the superconducting correlation length equals half the system size,  $\xi = 54a$  (2D) and  $\xi = 10.6a$  (3D), where  $a$  denotes the lattice spacing. Further computational details have been relegated to the Appendix.

*Results: Adatom site (2D and 3D).* On the adatom the local order parameter is greatly reduced with respect to the bulk value  $\Delta(\mathbf{r}) \sim 0.1\Delta_{\text{BCS}}$ . On the other hand, the experimentally accessible spectral gap on the adatom is enhanced in the same way as on the site below. We note that such an effect has been demonstrated before in disordered superconductors, where self-consistency leads to regions with low order parameter exhibiting a large spectral gap [5]. The spectral gap on the sites other than the adatom is comparable to the local order parameter.

*Results: Thin-film substrate (2D).* For our investigation we focus on the pairing response (to the adatom) of the metal atoms near the surface (substrate). Figure 2(a) displays the spatially resolved response of the pairing amplitude  $\Delta(\mathbf{r})$  near the impurity. Friedel oscillations with a frequency of  $2k_F$  are clearly visible, as one would have expected. Also, the superconducting gap is enhanced at the impurity site, in the computation by more than 24%.

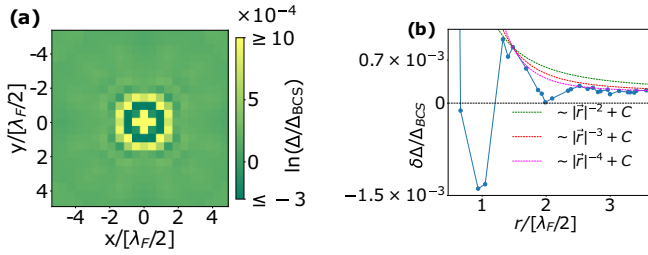


FIG. 3. (a) Spatial map of the logarithm of the pairing amplitude in the surface layer of a 3D superconductor with an impurity at the origin. (b) Response of the pairing amplitude to an impurity on the surface of a 3D superconductor. The response is computed from data shown in (a) averaged over the surface angle. The prefactors of the power-law fits are chosen such that they agree with the data at  $r = 1a \approx 1.48\lambda_F/2$ . (Parameters: filling  $n = 0.12$ ,  $U = 3.2$ ,  $V_{\text{imp}} = -0.06t$ ,  $\lambda_F/2 \approx 2.14a$ ,  $C \approx 1.8 \times 10^{-4} \Delta_{\text{BCS}}$ .)

In Fig. 2(b) the envelope of the oscillatory part of the pairing amplitude is analyzed. In order to highlight the  $1/r$ -type power-law decay, the product  $r\Delta(r)$  is plotted; it displays amplitude fluctuations with a strength independent of  $r$  as characteristic of a  $1/r$  envelope. Note that this behavior is in pronounced contrast to the familiar textbook result for the free Fermi gas, where we have the asymptotics  $\sin(2k_F r)/(k_F r)^d$  for particle-density oscillations in  $d$  dimensions, so  $1/r^2$  in 2D [20]. We mention that similar behavior has been detected in layered superconductors with anisotropic pairing, where the Ruderman-Kittel-Kasuya-Yosida (RKKY) interaction is comprised of a normal  $r^{-2}$  and a superconducting  $r^{-1}$  contribution [21].

*Results: Thick-film substrate (3D).* In Fig. 3, the pairing response (to the adatom at the origin) of the metal atoms at the surface (substrate) of a cube with a linear size  $L = 22$  sites is shown. The overall shape of the response is qualitatively similar to the 2D case. For instance, an enhancement of the gap by 20% is observed underneath the impurity site,  $\Delta(r = 0) = 1.2\Delta_{\text{BCS}}$  [22].

A significant difference with the thin-film response occurs with respect to the decay of the oscillations. In order to better highlight this important point, in Fig. 3(b) we plot the response (to adding the impurity) of the local gap function  $\delta\Delta(r)$  averaged over a circle with radius  $r$  around the impurity site. Due to the cubic symmetry underlying our microscopic model (and the simulation volume), the rotational symmetry is broken and therefore the integration over the circle reduces the oscillation amplitudes. Nevertheless, the  $2k_F$  oscillation is clearly visible in Fig. 3(b). As to the corresponding envelope function, we observe a significantly different thick-film decay compared to the thin-film limit. While for the system sizes available to us the true asymptotics is out of reach, strictly speaking, in the intermediate regime our data in Fig. 3 exhibit an envelope  $r^{-n_s} + C$  with  $n_s > 2$ ; the constant  $C$  depends on system size and is expected to vanish upon  $L \rightarrow \infty$ , ultimately revealing the true asymptotic decay. We take our observation as evidence that the surface exponent  $n_s$  exceeds the corresponding bulk exponent  $n_b$  that takes a known value  $n_b = 2$  [2].

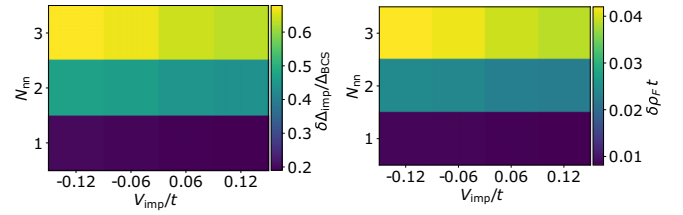


FIG. 4. Response of the superconducting gap  $\delta\Delta_{\text{imp}}$  (left) and the normal-state LDOS at the Fermi energy  $\delta\rho_F$  (right) to an impurity (adatom) located on the surface of the cubic lattice (same situation as in Fig. 3). Shown is the dependency on the impurity potential  $V_{\text{imp}}$  (horizontal axis) and the number of nearest neighbors  $N_{\text{nn}}$  of the impurity site (vertical axes).  $\delta\Delta_{\text{imp}}$  and  $\delta\rho_F$  quantify the average response of the gap and the normal-state LDOS at the Fermi energy on all sites neighboring the impurity. (Parameters: filling  $n = 0.12$ ,  $U = 3.2$ .)

*Gap and density.* We rationalize our results by recalling a basic result from BCS theory that connects the superconducting gap with the density of states at the Fermi surface  $\rho_F$ :

$$\Delta \simeq 2\hbar\omega_D e^{-\frac{1}{U\rho_F a^d}}. \quad (1)$$

Here, the pairing volume  $a^d$  relates the attractive Hubbard interaction  $U$  to the effective pairing interaction  $V_{\mathbf{k},\mathbf{k}'}$  featured by BCS theory. The latter binds a Cooper pair with energy density  $V$  if the corresponding particle-hole states are situated within a shell around  $E_F$  of width  $\hbar\omega_D$  (in the present model  $\hbar\omega_D \approx U$ ); hence  $a = v_F/\omega_D$  and  $V \sim Ua^d$ , introducing the Fermi velocity  $v_F$ . Reinterpreting Eq. (1) on a local scale, we stipulate an approximate relation

$$\ln \left[ \frac{\Delta(\mathbf{r})}{2\hbar\omega_D} \right] \simeq -\frac{1}{N(\mathbf{r})}, \quad (2)$$

where the abbreviation  $N(\mathbf{r}) := U\rho_F(\mathbf{r})a^d$  has the interpretation of the number of particles within the distance  $\sim U$  from  $E_F$  inside the correlation volume  $a^d$ . In the superconducting phase these particles participate in pair formation with a gap size exponentially decreasing with  $N^{-1}(\mathbf{r})$  increasing. These heuristic considerations prompt the formulation of a rule of thumb: A modulation of the LDOS at the Fermi energy in the normal phase is typically accompanied by a proportional modulation of the local gap function in the superconducting phase; in other words, particle densities  $n(\mathbf{r})$  slightly enhanced above the clean reference value correspond to slightly enhanced gap values  $\Delta(\mathbf{r})$ .

A numerical test of this proposition has been depicted in Fig. 4. For different kinds of binding scenarios—adatoms in on-site, bridge, and hollow positions ( $N_{\text{nn}} = 1, 2, 3$ )—and for varying on-site potential  $V_{\text{imp}}$ , the response of the gap and the normal-state density in the metal substrate near the impurity is shown. The conjectured rule of thumb manifests in the strong resemblance of left and right panels. Such a correlation between normal-state LDOS and the order parameter has been demonstrated before in superconductors with substitutional atom impurities [23].

This property of the increase of the LDOS at the Fermi energy below an adatom impurity distinguishes it from the case of a substitutional atom impurity, which has been studied

earlier [3,7,10–12]. In these studies a decrease of the superconducting gap at the impurity was found.

Furthermore, Fig. 4 shows that our results are only weakly dependent both on the sign and amplitude of the impurity potential, showing that the enhancement effect does not depend on fine tuning.

#### IV. CONCLUSIONS AND SUMMARY

Motivated by STM measurements of the superconducting gap near an adatom on an Al(111) surface, we have performed corresponding simulations within the BdG formalism. Our simulations capture all qualitative features seen in the experiment: (i) relatively quickly decaying Friedel oscillations (as compared to the thin-film limit studied in simulations); and (ii) an enhancement of the superconducting gap in the vicinity of the impurity of the order of 10%. The enhancement has been traced back to the modulation of the (normal-state) LDOS at the Fermi energy in the vicinity of the adatom. In recent experiments on FeSe superconductors with a finite impurity concentration, a global increase of the critical temperature has been observed [24]. It remains to be seen if the mechanism described in this Letter can have a similar effect.

Our results are encouraging in the sense that BdG has been shown to provide a reliable framework reproducing the salient features of physical reality, at least on a semiquantitative level. Future work should provide more detailed (and extensive) investigations comprising, in particular, a larger set of experimental realizations screening different substrates and adatoms.

#### ACKNOWLEDGMENTS

We are grateful to Igor Burmistrov and Christoph Strunk for numerous inspiring discussions and Thomas Gozlinzky for preparing some of the figures. We acknowledge funding from the Deutsche Forschungsgemeinschaft (DFG) with Grants No. Wu 394/12-1, No. INST 121384/30-1 FUGG, No. EV30/11-1, No. EV30/12-1, No. EV30/14-1, and No. SFB-1277 (Projects A03). We gratefully acknowledge the Gauss Centre for Supercomputing e.V. [25] for funding this project by providing computing time on the GCS Supercomputer SuperMUC at Leibniz Supercomputing Centre [26]. This work was performed on the supercomputer ForHLR funded by the Ministry of Science, Research and the Arts Baden-Württemberg and by the Federal Ministry of Education and Research.

#### APPENDIX

##### 1. Experimental background

###### *a. Experimental details*

A bulk Al crystal of (111) orientation was cleaned by cycles of Ar-ion sputtering and annealing to 700 K in UHV until clean and atomically flat surfaces were found with STM. After STM inspection, impurities in the form of Fe atoms were deposited onto the sample while resting in the STM at cryogenic temperatures [27,28]. The low mobility at these temperatures prohibits thermal diffusion and the Fe atoms do not aggregate to larger clusters or islands. At the base temperature of the

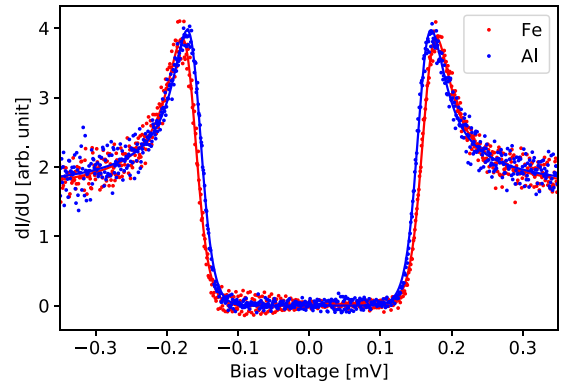


FIG. 5. Differential conductance  $dI/dU$  recorded at 25 mK on bare Al(111) (blue dots) and atop a single Fe atom on Al(111) (red dots) together with fits (solid lines) to thermally smeared BCS density of states. Blue and red solid lines display the fits to the experimental data points. Feedback conditions:  $U = 400 \mu\text{V}$ ,  $I = 500 \text{ pA}$ .

STM of  $\approx 25 \text{ mK}$  [15], spectra of the voltage-dependent tunneling current  $I(U)$  were recorded with the feedback loop of the STM disabled.  $dI/dU$  curves were obtained by a numerical derivative in order to avoid energy smearing when using a lock detection. STM tips were prepared from high-purity W wire by chemical etching and cleaning in UHV. The tips were not superconducting as tested by taking the tunneling spectra of a Au(111) surface at the base temperature.

###### *b. Gap enhancement with Fe impurity*

Figure 5 shows the tunneling spectra recorded on a clean area  $\approx 23 \text{ nm}$  away from Fe atoms (blue dots) and atop an Fe impurity (red dots). Fe is the most common impurity in Al and the absence of a Kondo effect in high-purity Al indicates that the magnetic moment of Fe in Al is absent from the beginning. To verify this, we drove Al to the normal phase by applying a magnetic field of 14 mT normal to the surface. While this field induces a transition to the normal state, it hardly is strong enough to eventually eliminate a possible Kondo resonance of the Fe spin. Nevertheless, we could not observe any Kondo peak in  $dI/dU$  spectra (not shown), in agreement with the nonmagnetic nature of Fe on Al(111). Thus with the absence of a magnetic moment of Fe in Al, we also do not expect to observe Yu-Shiba-Rusinov bound states [29–31], i.e., the Fe impurity does not break Cooper pairs by spin-flip scattering reducing the superconducting gap  $\Delta$  or inducing in-gap states. Even more,  $\Delta$  atop the Fe atoms appears larger than that on the bare Al(111) surface in the experiment (see Fig. 5).

Fitting the  $dI/dU$  spectra with thermally broadened BCS density of states [15] allowed us to quantify the increase from the bare Al gap of  $159.6 \pm 0.1 \mu\text{eV}$  to  $166.6 \pm 0.1 \mu\text{eV}$ , while the broadening of both curves due to the electronic temperature does not change significantly ( $112 \pm 1$  vs  $115 \pm 1 \text{ mK}$ ). We conclude that, while Fe acts as a local scatterer for electrons and presumably also Cooper pairs on the Al(111) surface, it does not act as a spin scatterer. Following this result, any scatterer on the surface or near the surface should induce similar local variations of the  $\Delta$  as evidenced for the buried defect in Fig. 1.

## 2. Computational model and method

We study the Bogoliubov–de Gennes (BdG) model with an adatom impurity

$$\hat{H} = \hat{H}_{\text{BdG}} + \hat{H}_{\text{imp}}, \quad (\text{A1})$$

where

$$\begin{aligned} \hat{H}_{\text{BdG}} = & -t \sum_{\langle i,j \rangle, \sigma} \hat{c}_{i,\sigma}^\dagger \hat{c}_{j,\sigma} - \sum_{i=1, \sigma}^{N_{\text{lat}}} \left( \frac{U}{2} n(\mathbf{r}_i) + \mu \right) \hat{n}_{i,\sigma} \\ & + \sum_{i=1}^{N_{\text{lat}}} U \langle \hat{c}_{i,\downarrow}^\dagger \hat{c}_{i,\uparrow}^\dagger \rangle \hat{c}_{i,\uparrow} \hat{c}_{i,\downarrow} + \text{H.c.} \end{aligned} \quad (\text{A2})$$

The impurity is realized as an extra site external to the Hubbard lattice,

$$\begin{aligned} \hat{H}_{\text{imp}} = & -t \hat{c}_{L,\sigma}^\dagger \hat{c}_{1,\sigma} - \left( \frac{U}{2} n(\mathbf{r}_l) + \mu - V_{\text{imp}} \right) \hat{n}_{l,\sigma} \\ & + U \langle \hat{c}_{L,\downarrow}^\dagger \hat{c}_{L,\uparrow}^\dagger \rangle \hat{c}_{L,\uparrow} \hat{c}_{L,\downarrow} + \text{H.c.}, \end{aligned} \quad (\text{A3})$$

with local occupation number  $n(\mathbf{r}_i) = \sum_{\sigma} \langle \hat{n}_{i,\sigma} \rangle$ , pairing amplitude  $\Delta(\mathbf{r}_i) = \langle \hat{c}_{i,\downarrow}^\dagger \hat{c}_{i,\uparrow}^\dagger \rangle$ ,  $U > 0$ , number of lattice sites  $N_{\text{lat}}$ , and impurity of potential  $V_{\text{imp}}$  at site  $\mathbf{r}_l$ . All computations are conducted at  $T = 0$ ; the chemical potential  $\mu$  is adjusted to fix the particle density  $\sum_i \frac{n(\mathbf{r}_i)}{N_{\text{lat}}} = n$ . In the case of the 2D system  $\hat{H}_{\text{BdG}}$  is defined on a periodic square lattice of linear size  $L = 121a$ , with lattice constant  $a$ . In 3D the cubic lattice that  $\hat{H}_{\text{BdG}}$  is defined on, is periodic in the  $x$  and  $y$  axis, whereas on the  $z$  axis we impose open boundary conditions. In 3D the linear system size is  $L = 22$ . The adatom is located on one of the surfaces. The density  $n(\mathbf{r})$  and pairing amplitude  $\Delta(\mathbf{r})$  are computed self-consistently up to tolerance  $\alpha = 10^{-5}$  in Fig. 2 and  $\alpha = 10^{-6}$  in Fig. 3.  $\Delta(\mathbf{r})$  will be given in units of the clean gap  $\Delta_{\text{BCS}}$  without the impurity. To compute the response, we take the difference of the self-consistent potentials with and without impurity excluding the impurity site. For a more in-depth description of the solution of the BdG system, we refer to Ref. [32]. All results have been computed with a full-diagonalization solver.

- 
- [1] J. Friedel, *London, Edinburgh Dublin Philos. Mag. J. Sci.* **43**, 153 (1952).
- [2] A. L. Fetter, *Phys. Rev.* **140**, A1921 (1965).
- [3] K. Tanaka and F. Marsiglio, *J. Phys. Chem. Solids* **63**, 2287 (2002).
- [4] A. Ghosal, M. Randeria, and N. Trivedi, *Phys. Rev. Lett.* **81**, 3940 (1998).
- [5] A. Ghosal, M. Randeria, and N. Trivedi, *Phys. Rev. B* **65**, 014501 (2001).
- [6] K. Machida and F. Shibata, *Prog. Theor. Phys.* **47**, 1817 (1972).
- [7] M. E. Flatté and J. M. Byers, *Phys. Rev. B* **56**, 11213 (1997).
- [8] A. V. Balatsky, I. Vekhter, and J.-X. Zhu, *Rev. Mod. Phys.* **78**, 373 (2006).
- [9] E. G. Dalla Torre, D. Benjamin, Y. He, D. Dentelski, and E. Demler, *Phys. Rev. B* **93**, 205117 (2016).
- [10] L. Lauke, M. S. Scheurer, A. Poenicke, and J. Schmalian, *Phys. Rev. B* **98**, 134502 (2018).
- [11] K. Tanaka and F. Marsiglio, *Physica C* **384**, 356 (2003).
- [12] W.-F. Tsai, Y.-Y. Zhang, C. Fang, and J. Hu, *Phys. Rev. B* **80**, 064513 (2009).
- [13] Y. Hasegawa and P. Avouris, *Phys. Rev. Lett.* **71**, 1071 (1993).
- [14] M. Schmid, G. Leonardelli, R. Tscheliebnig, A. Biedermann, and P. Varga, *Surf. Sci.* **478**, L355 (2001).
- [15] T. Balashov, M. Meyer, and W. Wulfhekel, *Rev. Sci. Instrum.* **89**, 113707 (2018).
- [16] S. J. Sferco, P. Blaha, and K. Schwarz, *Phys. Rev. B* **76**, 075428 (2007).
- [17] Y. Shihara, M. Kohyama, and S. Ishibashi, *Phys. Rev. B* **81**, 075441 (2010).
- [18] W. A. Harrison, *Phys. Rev.* **116**, 555 (1959).
- [19] C. Kittel, *Introduction to Solid State Physics* (Wiley, New York, 1996).
- [20] G. Giuliani, *Quantum Theory of the Electron Liquid* (Cambridge University Press, Cambridge, UK, 2005).
- [21] D. N. Aristov, S. V. Maleyev, and A. G. Yashenkin, *Z. Phys. B* **102**, 467 (1997).
- [22] We mention that we have tested our results against model assumptions. Specifically, the gap enhancement underneath the impurity changes only in the per-mille regime upon changing the value of the on-site interaction of the iron impurity from attractive ( $U = 3.2t$ ) to repulsive ( $U = 0.0t$ ,  $U = -3.2t$ ).
- [23] M. N. Gastiasoro and B. M. Andersen, *Phys. Rev. B* **98**, 184510 (2018).
- [24] S. Teknowijoyo, K. Cho, M. A. Tanatar, J. Gonzales, A. E. Böhmer, O. Cavani, V. Mishra, P. J. Hirschfeld, S. L. Bud'ko, P. C. Canfield, and R. Prozorov, *Phys. Rev. B* **94**, 064521 (2016).
- [25] [www.gauss-centre.eu](http://www.gauss-centre.eu).
- [26] [www.lrz.de](http://www.lrz.de).
- [27] M. F. Crommie, C. P. Lutz, and D. M. Eigler, *Science* **262**, 218 (1993).
- [28] T. Miyamachi, T. Schuh, T. Märkl, C. Bresch, T. Balashov, A. Stöhr, C. Karlewski, S. André, M. Marthaler, M. Hoffmann, M. Geilhufe, S. Ostanin, W. Hergert, I. Mertig, G. Schön, A. Ernst, and W. Wulfhekel, *Nature (London)* **503**, 242 (2013).
- [29] L. Yu, *Acta Phys. Sin.* **21**, 75 (1965).
- [30] H. Shiba, *Prog. Theor. Phys.* **40**, 435 (1968).
- [31] A. Rusinov, *Zh. Eksp. Teor. Fiz., Pis'ma Red.* **9**, 146 (1968).
- [32] M. Stosiek, B. Lang, and F. Evers, *Phys. Rev. B* **101**, 144503 (2020).